International Journal of Biochemistry and Cell Biology 114 (2019) 105569

Contents lists available at ScienceDirect

International Journal of Biochemistry and Cell Biology

journal homepage: www.elsevier.com/locate/biocel

Genetically targeted fluorescent probes reveal dynamic calcium responses to adrenergic signaling in multiple cardiomyocyte compartments

Ivan Luptak[a], Robert Morgan[a], Tomas Baka[b], Dominique Croteau[a], Daniel Moverman[a], Hannah Sarnak[a], Michael Kirber[c], Markus M. Bachschmid[d], Wilson S. Colucci[a], David R. Pimentel[a,*]

[a] Myocardial Biology Unit, Boston University School of Medicine, Boston, MA, United States
[b] Institute of Pathophysiology, Faculty of Medicine, Comenius University, Bratislava, Slovakia
[c] Cellular Imaging Core, Boston University School of Medicine, Boston, MA, United States
[d] Vascular Biology Unit, Boston University School of Medicine, Boston, MA, United States

ARTICLE INFO

Keywords:
FRET imaging
Calcium signaling
Cellular compartments
Mitochondrial calcium
Cameleon
Mitochondrial calcium uniporter dominant negative

ABSTRACT

Calcium (Ca^{2+}), an important second messenger, regulates many cellular activities and varies spatiotemporally within the cell. Conventional methods to monitor Ca^{2+} changes, such as synthetic Ca^{2+} indicators, are not targetable, while genetically encoded Ca^{2+} indicators (GECI) can be precisely directed to cellular compartments. GECIs are chimeric proteins composed of calmodulin (or other proteins that change conformation on Ca^{2+} binding) coupled with two fluorescent proteins that come closer together after an increase in [Ca^{2+}], and enhance Förster resonance energy transfer (FRET) that allows for ratiometric [Ca^{2+}] assessment. Here, adult rat ventricular myocytes were transfected with specifically targeted calmodulin-based GECIs and Ca^{2+} responses to a physiological stimulus, norepinephrine (NE, 10 μM), were observed in a) sarcoplasmic reticulum (SR), b) mitochondria, c) the space between the mitochondria and SR, termed the Mitochondria Associated Membrane space (MAM) and d) cytosol for 10 min after stimulation. In SR and mitochondria, NE increased the [Ca^{2+}] ratio by 17% and by 8%, respectively. In the MAM the [Ca^{2+}] ratio decreased by 16%, while in cytosol [Ca^{2+}] remained unchanged. In conclusion, adrenergic stimulation causes distinct responses in the cardiomyocyte SR, mitochondria and MAM. Additionally, our work provides a toolkit-update for targeted [Ca^{2+}] measurements in multiple cellular compartments.

1. Introduction

In contractile tissues such as skeletal muscle or myocardium, large amplitude cytosolic Ca^{2+} cycling, responsible for the regulation of contraction and relaxation, have been well described using a variety of indicators (Paredes et al., 2008). However, assessment of calcium dynamics between different subcellular compartments is crucial for understanding the role of Ca^{2+} in normal and pathological cell signaling and function (Balaban, 2009; Boyman et al., 2015; Brookes et al., 2004; Chami et al., 2008; Csordás and Hajnóczky, 2009; Liu and O'Rourke, 2009; Luptak et al., 2018, 2005; Raffaello et al., 2016; Santulli et al., 2015). Assessment of these low amplitude, low frequency Ca^{2+} transients on the background of large oscillation of cytosolic free [Ca^{2+}] has been particularly challenging (Berridge et al., 2003; Bers, 2008).

Ca^{2+} indicators fall into two major categories: a) synthetic Ca^{2+} indicators (such as fura-2, indo1, fluo-3, calcium green) and b) genetically-encoded Ca^{2+} indicators (GECI) (Palmer and Tsien, 2006). The synthetic indicators are suitable for assessment of cytosolic [Ca^{2+}] due to their large dynamic ranges, but they cannot be targeted to specific cellular compartments and lack sensitivity in measuring low nanomolar concentrations of calcium (Paredes et al., 2008). In contrast, GECIs can be directed to specific cellular compartments, and be used to assess nanomolar [Ca^{2+}] ranges (Horikawa et al., 2010). Of the GECIs, the Cameleons, that utilize calmodulin and Förster resonance-energy transfer (FRET) (Miyawaki et al., 1997; Palmer et al., 2006; Palmer and Tsien, 2006), collectively have the largest detection range of Ca^{2+} encompassing low nanomolar (K_d 15 nM) to micromolar concentrations (K_d 64 μM). Cameleons are chimeric proteins that change conformation to Ca^{2+} binding and increase FRET between two fluorescent proteins. This allows for convenient ratiometric Ca^{2+} fluorescent assessment (Miyawaki et al., 1997; Palmer et al., 2006; Palmer and Tsien, 2006).

To evaluate the role of calcium in cardiomyocyte compartments, we

* Corresponding author at: Cardiovascular Medicine Section, Boston University Medical Center, 88 E Newton St, Boston, MA 02118, United States.
E-mail address: dapiment@bmc.org (D.R. Pimentel).

https://doi.org/10.1016/j.biocel.2019.105569
Received 9 March 2019; Received in revised form 5 July 2019; Accepted 7 July 2019
Available online 09 July 2019

designed Cameleon probes to allow calcium imaging in: a) sarcoplasmic reticulum (SR), b) mitochondria, c) the space between the mitochondria and SR, termed the Mitochondria Associated Membrane space (MAM), and d) cytosol. For each compartment, the response to caffeine-induced SR Ca^{2+} release was used to determine the appropriate sensitivity for Ca^{2+} detection.

In cardiomyocytes, norepinephrine (NE), a well-established physiological stimulus, induces robust inotropic and lusitropic effects associated with Ca^{2+} channels, phospholamban and troponin I phosphorylation (Bers, 2002; Mayourian et al., 2018). As these effects of norepinephrine are driven by alpha- and beta-adrenoceptor activation, we used alpha- and beta-adrenoceptor antagonists (prazosin and propranolol, respectively) to reveal the contribution of NE's effect on subcellular [Ca^{2+}] responses. To date, a complex evaluation of signaling Ca^{2+} responses to a single stimulus (e.g. NE) in multiple subcellular compartments has not been achieved in cardiomyocytes.

In summary, we characterized Ca^{2+} changes in subcellular compartments in response to NE in primary cultures of adult rat ventricular myocytes (ARVM) (Ellingsen et al., 1993; Kuster et al., 2005). Furthermore, by using an updated toolkit for targeted [Ca^{2+}] measurements in various compartments, we show that this approach allows Ca^{2+} measurements in multiple cells simultaneously.

2. Methods

2.1. Cell culture

ARVMs were isolated from the hearts of adult (200 to 220 g) male Sprague-Dawley rats as described previously (Kuster et al., 2005).

2.2. Cell treatments

L-Norepinephrine (10 μmol/L; Sigma) was added immediately before measurements. In some experiments, DL-Propranolol (2 μmol/L; Sigma) or Prazosin (100 nmol/L; Sigma) were added 60 min before L-norepinephrine. Ascorbic acid (100 μmol/L; Sigma) was added to prevent oxidation of L-norepinephrine. Thapsigargin (5 μmol/L; Sigma) was added 10 min prior to experiments.

2.3. Adenoviral constructs

The plasmid encoding mitochondrial calcium uniporter (MCU) was obtained from Addgene clone 31,726 (Baughman et al., 2011). The 3-threonine amino acid was changed to an alanine to match the reference sequence and a stop codon was added. Using site directed mutagenesis, amino acids D261 and E264 were both changed to glutamine, which leads to a dominant negative mitochondrial calcium uniporter (DNMCU) (Rasmussen et al., 2015). A primer of tgaagtatgttactggctg-catgatctgcc-aggaatattcccacca and its reverse complement were used for the mutagenesis reaction. The clone was confirmed by sequencing (Genewiz). An adenovirus was created using the AdEasy system and β-galactosidase was used as control as previously described (Pimentel et al., 2006). All calcium biosensor adenoviral constructs were created using the AdEasy system as well.

2.4. Cloning of Cameleon-based Ca^{2+} biosensors targeted to various cellular compartments

Cameleon clones with K_d of 1 u M (D1) (Palmer and Tsien, 2006), ˜600 nM (D3) (Palmer and Tsien, 2006), 64 μM (D4 Addgene clone 37,473) (Palmer et al., 2006), 140 nM (Addgene clone 51966- yellow Cameleon-Nano 140) (Horikawa et al., 2010), and 15 nM (Addgene clone 51961- yellow Cameleon-Nano 15) (Horikawa et al., 2010) were used as the reporter constructs. Together, we will refer to these as Cameleon clones. To target particular compartments, we cloned or subcloned the following sequences: (1) The MAM targeting sequence was cloned from total C57BL/6 J mouse cardiac mRNA and consisted of the first 67 AA of the DGAT2 sequence (Stone et al., 2009). The forward sequencing primer was "gtgacgtgcattggcttcag" and reverse "cctagcaccaggaaggatagg" (2). The mitochondrial targeting sequence with four copies of the subunit VIII of human cytochrome C oxidase (Palmer and Tsien, 2006) was sub-cloned from the mitoD3CPV (kind gift from R.Y.Tsien) (3). The SR targeting sequence was sub-cloned from the D1ER clone (kind gift from R.Y.Tsien) (Palmer and Tsien, 2006) and sub-cloned onto D3CPV and 140K_d clones with a C-terminal KDEL sequence attached on each using PCR. All cloning and sequencing primers were supplied by Fisher. All clones were sequenced to ensure the appropriate sequences were obtained.

2.5. Cell imaging

ARVMs were transfected for 48 h and then imaged at 37 °C using an inverted Olympus Spinning Disk confocal microscope in wide field mode. The light source was Prior Lumen Pro 220. All optical filters were obtained from Chroma: excitation 436/20 nm, dichroic 455 L P, emission YFP 535/30 nm, emission CFP 480/40 nm. The cardiac myocytes were localized with light microscopy and subsequently visualized for fluorescence excited at 426–446 nm while data from CFP and YFP emission were collected using a rapid emission filter changer (Prior). All images were taken with a plan-apochromatic 20x/0.4NA (Olympus). Data were analyzed using NIS Elements software (Nikon). Ratiometric images were calculated using background-subtracted YFP emission divided by background-subtracted CFP emission. Cells were observed over a period of 20 s with image acquisition every second after caffeine (20 mM) administration. Cells were observed over a period of 10 min with image acquisition every 20–30 s after NE (10 μM) in the presence and absence of propranolol (2 μM) and/or prazosin (100 nM). Only rod-shaped cardiomyocytes were included in the analysis.

To prove the correct localization of the probes 100 nM of ER-Tracker Red (Invitrogen) and Mito-Tracker Red FM (Invitrogen) were added for 15 min and washed immediately prior to imaging. Red localization dyes were needed as the FRET probes' emission wavelengths overlap with green fluorescent imaging. For the localization of the SR and MAM probes, structured illumination microscope (SIM) images were acquired using the Nikon N-SIM super resolution system and a SR Apo TIRF 100 × 1.49NA objective (Nikon Instruments, Melville, NY). SIM image processing was performed using the previously published 3D reconstruction methodology (Gustafsson et al., 2008) and NIS-Elements software. For the localization of the mitochondrial probe confocal imaging was performed using a LSM710 system (Zeiss, Thornwood, NY). All images were taken with a Plan-Apochromat 100 ×/1.4NA oil objective (Zeiss). The 488 nm argon laser line was used for imaging YFP. Emitted fluorescence was collected in the range of 507–549 nm. Excitation of Mito-Tracker was performed using the 543 nm laser. Emission was collected in the range of 561–735 nm. For further confirmation of localization of the endoplasmic reticulum probe confocal imaging was performed using Leica SP5 Confocal Microscope (Leica, Buffalo Grove, IL). All images were taken with a Plan-Apochromat 63 ×/1.4NA oil objective (Leica). The 405 nm argon laser line was used for imaging YFP. Emitted fluorescence was collected in the range of 464–600 nm. Excitation of ER-tracker Red was performed using the 594 nm laser. Emission was collected in the range of 603–700 nm. The cytosolic probe was localized using an Olympus microscope with a Plan-Apochromatic 60 ×/0.85NA objective (Olympus) and emission YFP 535/30 nm.

2.6. Determination of the correct Cameleon Ca^{2+} affinity for the individual cellular compartments

The correct K_d for each subcellular compartment was determined with caffeine-induced SR Ca^{2+} release. Caffeine rapidly depletes the SR of Ca^{2+} leading to a dramatically increased cytosolic (Bers, 2008) and

mitochondrial Ca^{2+} levels (Pan et al., 2013). The probes were tested for caffeine responsiveness at varying K_d levels based on prior literature reports (Horikawa et al., 2010; Palmer et al., 2006; Palmer and Tsien, 2006). Caffeine (20 mM) was rapidly administered and the cells were imaged every second for a total of 20 s. For probes directed to cellular compartments where caffeine increases [Ca^{2+}] (mitochondria and MAM), the lowest K_d clone that was still responsive to caffeine was used for the experiments. Conversely, for the SR probe, caffeine is expected to decrease SR [Ca^{2+}], and the reciprocal approach was taken: the highest K_d probe that still reacted to caffeine was selected for further use. (Fig. 2A).

2.7. Calibration of the cameleon probes

For calibration, cardiomyocytes were incubated in a potassium phosphate Hepes solution (in mM): Hepes (20), KCl (140), $MgCl_2$ (1.51), KH_2PO_4 (0.5), BAPTA (5) and BAPTA-AM (0.01) set at pH = 7.4 with KOH for cytosolic probe and pH = 8 for the mitochondrial probe to mimic the pH in mitochondrial matrix. The R_{min} was determined after membrane permeabilization. The R_{max} was reached by adding small volumes of $CaCl_2$ (10 or 50 mM stock) in stepwise manner to generate the calibration curve (Wüst et al., 2017). After conversion of the x-axis to logarithmic scale, the dose-response curve was fitted using GraphPad Prism software and 50% effective [Ca^{2+}] (EC50) was calculated for each probe. Fitted curves were shown with ± 95% confidence interval boundaries (Fig. 4).

2.8. Statistical analysis

Results are presented as mean ± SEM. Comparisons between groups were performed using unpaired t-tests, Mann-Whitney non-parametric tests or 2-way or repeated measures ANOVA, as appropriate. All statistical analyses were performed using GraphPad Prism software. P-value < 0.05 was considered significant.

3. Results

3.1. Localization of the cameleon probes

For SR localization, we used the calsequestrin targeting sequence from D1ER (Palmer and Tsien, 2006) in conjunction with a C-terminal KDEL retention sequence. Confocal microscopy showed overlap (Fig.1 **panel A3**) between the D3 ER probe **(**Fig.1 **panel A1)** and ER-tracker **(**Fig.1 **panel A2)**. In addition, high resolution SIM imaging confirmed the placement of the ER-Tracker that binds to the sulfonylurea receptors on the outside of the SR membrane. In the image shown (Fig. 1B), the Cameleon probe in the SR lumen is surrounded by the ER-Tracker on the outside of the SR membrane proving appropriate localization of the Ca^{2+} sensing probe. Caffeine was administered and diminution of the ratio was measured. We found that the D3 probe responded appropriately to caffeine and had a dual measured K_d = 793 nM and 1.85 mM (Fig. 4A).

For mitochondrial localization, we assessed the use of single to multiple copies (Filippin et al., 2005) of the targeting sequence from subunit VIII of human cytochrome C oxidase and found that a 4x leader sequence was required for successful localization of the probe to the mitochondria (Fig. 1C). Similar strategies to promote mitochondrial targeting have been used previously (Wüst et al., 2017). To search for the correct Ca^{2+} affinity of the mitochondrial probe, a similar iterative process to the ER probe was necessary. Despite the correct localization confirmed by SIM imaging (Fig. 1C), higher K_d Cameleon probes were minimally responsive to caffeine but the Cameleon probe with an *in vitro*-reported K_d = 15 nM still maintained responsivity to caffeine (Fig. 2B). Our calibration showed that the K_d of the probe when localized to the mitochondrial matrix of our cell type is about 6-fold higher, (EC50 91 ± 6 nM) (Fig.4B), and this value is similar to previously reported mitochondrial matrix Ca^{2+} levels using a different probe (Wüst et al., 2017).

Since the interplay between SR and mitochondria is important in the regulation of mitochondrial [Ca^{2+}] (Raffaello et al., 2016), we also targeted a Cameleon probe to the SR-mitochondrial space, termed the Mitochondrial Associated Membrane (MAM) space. Using the DAGT2 leader sequence, the probe was targeted to and localized in the MAM space (Stone et al., 2009) as confirmed by SIM imaging (Fig1**, D and E**). The Cameleon probe with a K_d = 15 nM was reactive to caffeine in this region. The actual K_d for this probe when calibrated in our cells was found to be more than 6-fold higher (EC50 132.2 ± 6.9 nM) (Fig.4C).

Lastly, no targeting sequence was needed for cytosolic localization. Similar to the mitochondrial and MAM probes, we found that the probe with K_d 15 nM was reactive to caffeine. Our calibration for the cytosolic probe revealed an estimated K_d ~60–80 nM which is consistent with previously reported values for cytosolic calcium concentrations (Boyman et al., 2013) (Fig. 4D).

3.2. NE increases free Ca^{2+} in the SR

After stimulation with NE for 10 min, the calcium fluorescence ratio in the SR increased by 16.5 ± 2.7% vs. baseline (Fig. 3A). Propranolol inhibited the NE-stimulated increase in Ca^{2+} ratio by 73%, whereas the alpha-adrenergic inhibitor, prazosin, caused a small, non-significant decrease. The use of both inhibitors almost completely (~ 90%) prevented the Ca^{2+} uptake by SR after stimulation with NE.

3.3. NE increases free Ca^{2+} in the mitochondria

As visualized with the mitochondria-directed probe, NE increased mitochondrial calcium ratio by 7.8 ± 1.0%. The increase was evident already at 60 s after NE application, and preceded the increase we observed in SR which occurred over 10 min. Propranolol inhibited the NE-induced increase in mitochondrial Ca^{2+} by 86%. There was a small non-significant inhibition by prazosin, and the combination of propranolol and prazosin almost completely inhibited the increase (Fig. 3B). This suggests mostly direct activation of calcium entry to mitochondria unrelated to SERCA activation by NE.

3.4. NE decreases free Ca^{2+} in the mitochondrial associated membrane (MAM) space

In contrast to the NE-stimulated increases observed in the SR and mitochondria, the calcium ratio in the MAM space decreased by 15.8 ± 1.4% (Fig. 3D). Similar to the NE-stimulated increases in the SR this effect was most evident after 10 min since NE application and was decreased by propranolol (73%), with only a non-significant decrease with prazosin and almost complete inhibition by the combination of propranolol and prazosin. To elucidate the contribution of both SERCA uptake and mitochondrial Ca^{2+} uptake to the decrease of Ca^{2+} in MAM space, we inhibited these with either thapsigargin or mitochondrial calcium uniporter (MCU) dominant negative viral construct (DNMCU), respectively (Fig. 3E**).** NE decreased the calcium ratio by 16.0 ± 0.9%. Inhibition with thapsigargin attenuated the Ca^{2+} decrease by 55% (to 9.1 ± 0.6%, $p < 0.0001$**).** DNMCU expression attenuated the Ca^{2+} decrease by 25% (to 12 ± 0.6%, $p < 0.01$**).** Inhibition of both reduced the Ca^{2+} uptake from MAM further, by 62% (to 6.1 ± 0.4%, $p < 0.0001$**)** (Fig. 3E**).** Thus, both Ca^{2+} uptake by SERCA and mitochondrial uptake via MCU seem to be important mechanisms mediating the decrease in MAM [Ca^{2+}] after adrenergic stimulation.

3.5. NE does not alter Ca^{2+} in the cytosol

Overexpression of the probe with no leader sequence resulted in diffuse distribution in the cytosol. NE caused no change in cytosolic

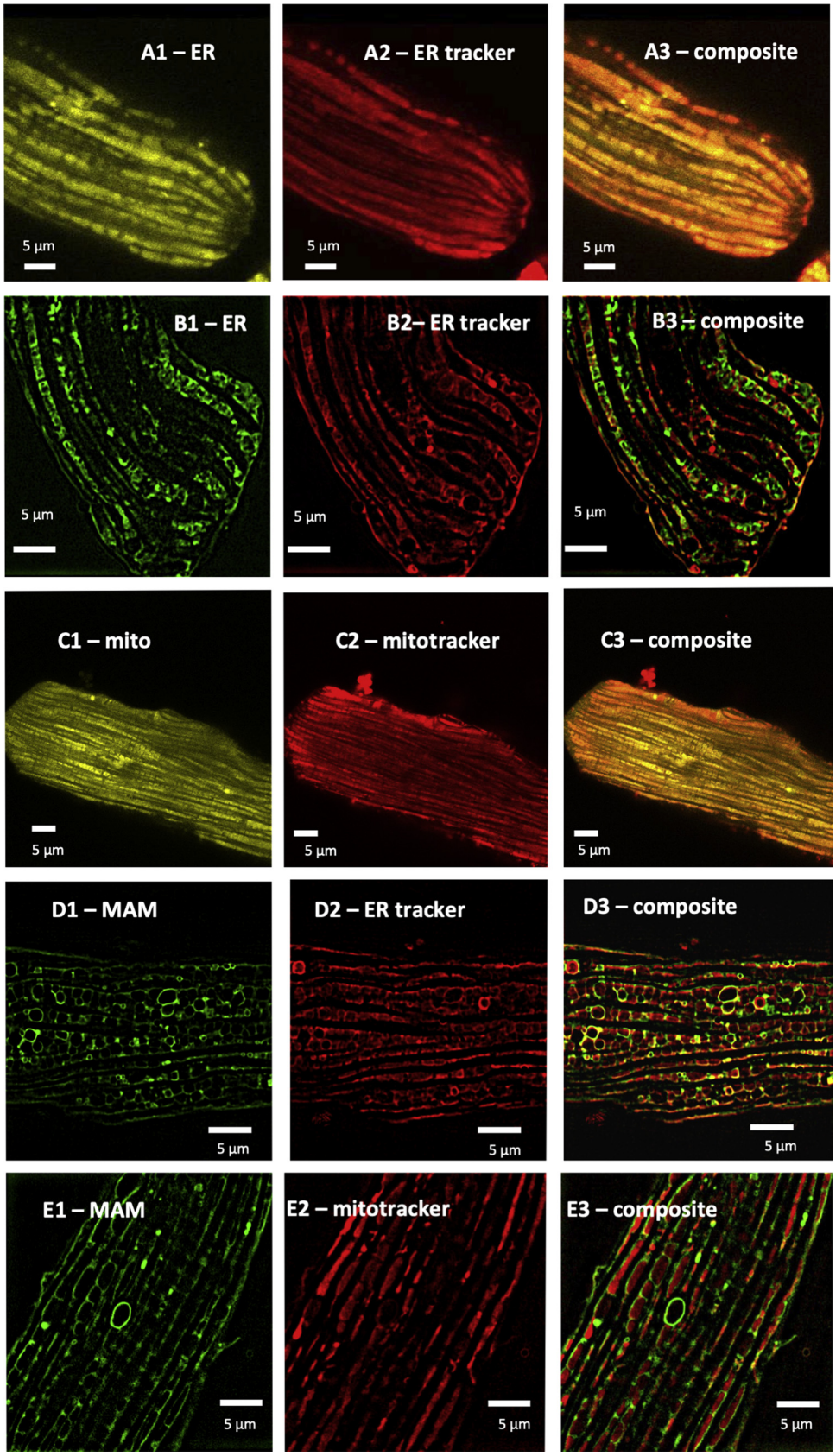

Fig. 1. Localization of the Cameleon probes to subcellular compartments in cardiomyocytes. (A and B): For *SR localization,* we utilized an N-Terminal calreticulin leader sequence coupled with a KDEL C-terminal sequence to place the probe in the ER lumen. In (A) overlap with ER-tracker Red is shown by confocal microscopy, in (B) co-localization with ER tracker, which binds to receptors on the outside of the ER, is shown by SIM imaging. **(C):** For *mitochondrial localization*, we found that a 4x leader sequence of cytochrome C oxidase was required to target the probe to a mitochondria. *Co-localization with Mitotracker* Red is shown. **(D) and (E):** For *mitochondrial associated membrane (MAM)* space, the leader sequence for DGAT2, a protein that has been reported to be present in the mitochondrial membrane space (MAM) was used. In **(D)** co-*localization with ER-tracker* Red is shown, in **(E)** co-*localization with Mitotracker* is shown.

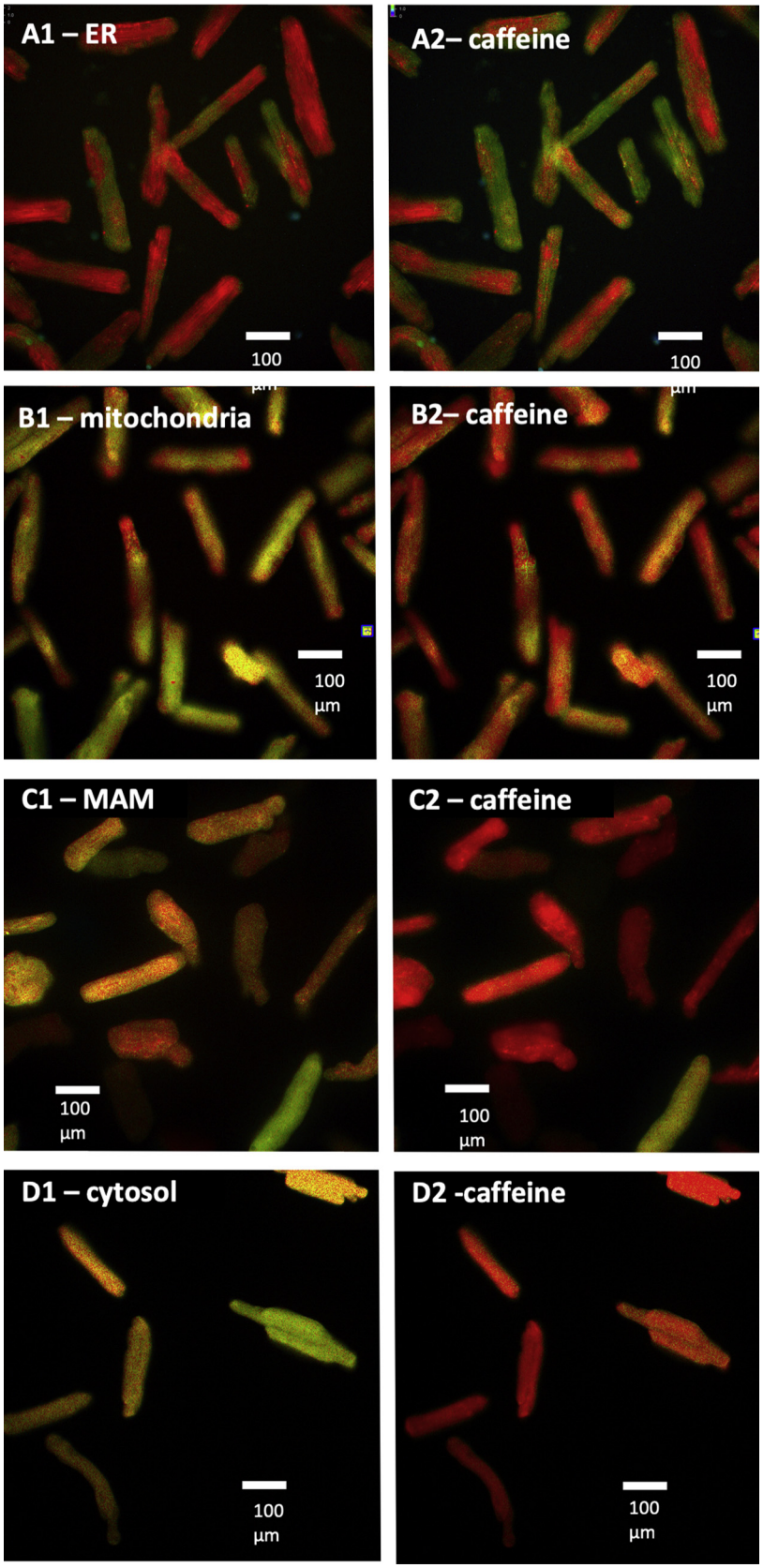

Fig. 2. Responses of the Cameleons to caffeine-induced SR calcium release in different cellular sub-compartments. Only rod-shaped cardiomyocytes were included in the analysis. Green color represents the lowest ratio (lowest [Ca^{2+}]), red color represents the highest ratio (highest [Ca^{2+}]). **(A)** endo-/sarcoplasmic reticulum (ER), *decrease* in [Ca^{2+}]; **(B)** mitochondria, *increase* in [Ca^{2+}] within 3 s; and **(C)** MAM, *increase* in [Ca^{2+}] within 3 s. **(D)** cytosol, *increase* in [Ca^{2+}] within 4 s. (For interpretation of the references to color in this figure legend, the reader is referred to the web version of this article).

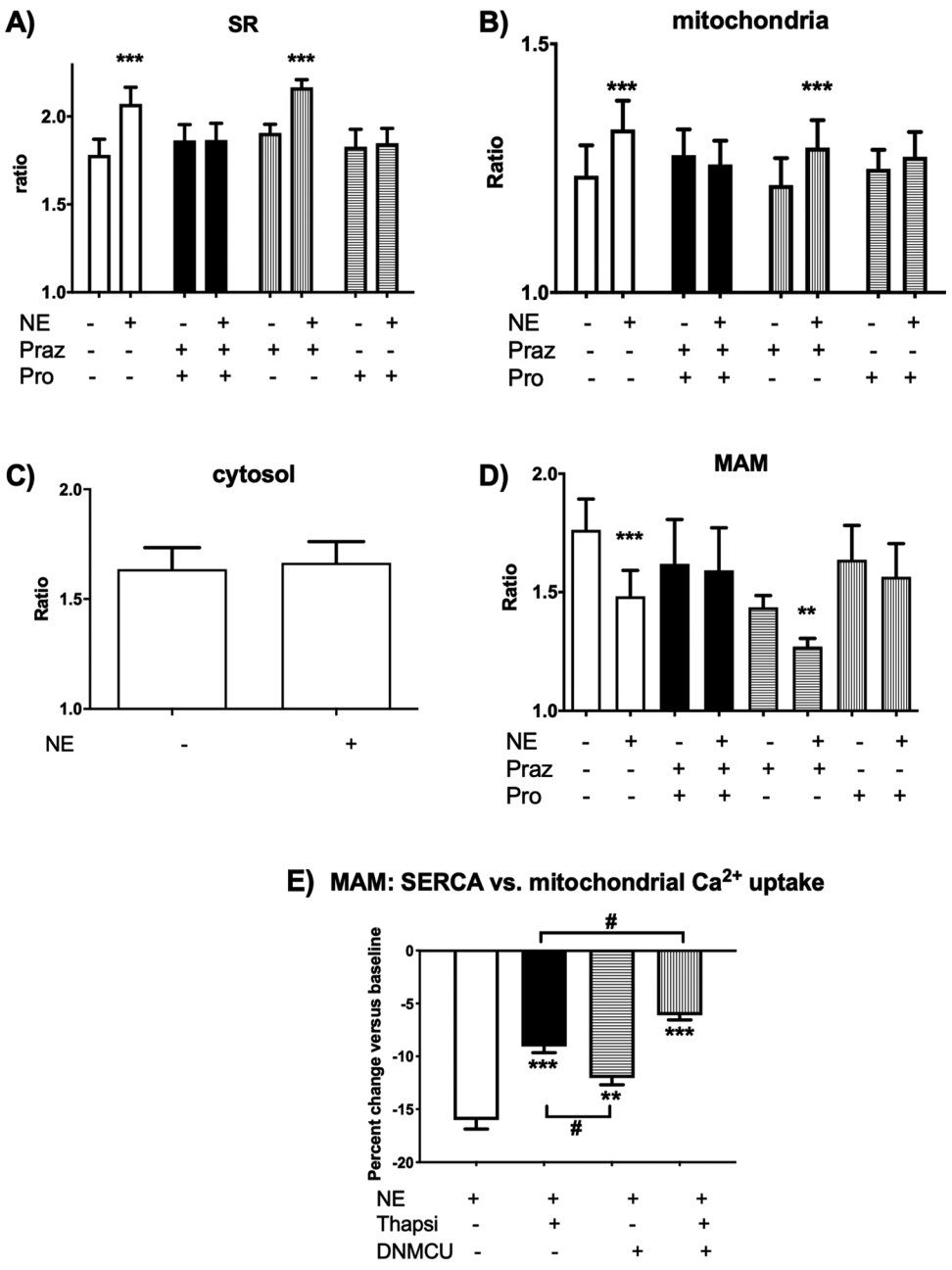

Fig. 3. Changes in free [Ca^{2+}] to 10 μM norepinephrine (NE): (A) SR [Ca^{2+}] increases. Cameleon Ca^{2+} ratio in SR increased by 16.5 ± 2.7% compared to baseline after the stimulus. Inhibition with propranolol (Pro) reduced the signal by 89% while the reduction of the NE response by an alpha-adrenergic inhibitor, prazosin (Praz) was not statistically significant. The use of both inhibitors (Praz + Pro) completely prevents the uptake of calcium by SR after stimulation with NE. **(B) Mitochondrial [Ca^{2+}] increases.** NE increased mitochondrial free [Ca^{2+}] by 8%. Dual adrenergic receptor inhibition (Praz + Pro) completely prevented the uptake and beta-adrenergic inhibitor propranolol (Pro) almost completely prevented the increase. **(C) Cytosolic [Ca^{2+}] remains unchanged after norepinephrine (NE).** The Ca^{2+} ratio of the Cameleon K_d probe overexpressed in the cytosol did not change within 10 min after the stimulus with 10 μM concentration of NE. **(D) MAM [Ca^{2+}] decreases.** NE decreased Cameleon Ca^{2+} ratio in the mitochondrial associated membrane (MAM) space by 8%. The NE Ca^{2+} signal in MAM was almost completely (by 90%) prevented by dual inhibition of the beta- and alpha-receptors (Praz + Pro): a) Beta-adrenergic blockade (Pro) prevents the Ca^{2+} decrease by 73% while b) prazosin (Praz) alone has no significant effect. **(E) MAM [Ca^{2+}] decrease is attenuated by inhibition of SERCA and mitochondrial Ca^{2+} uptake.** NE decreased the calcium ratio in MAM by 16%. Inhibition with thapsigargin 5 μM (Thapsi) attenuated the Ca^{2+} decrease by 55%. DNMCU expression attenuated the Ca^{2+} decrease by 25%. Inhibition of both reduced the Ca^{2+} uptake from MAM by 62%. (n = 5–7, ***p < 0.001, ** p < 0.01 vs control; #p < 0.05 vs. groups as outlined).

Ca^{2+} ratio over 10 min (Fig. 3C).

4. Discussion

The Ca^{2+} transients responsible for excitation-contraction coupling have been well described using small molecule Ca^{2+} indicators in the cytosol (Bers, 2008). However, in addition to these large cytosolic Ca^{2+} transients, there are smaller Ca^{2+} movements within the localized regions of the cell (Berridge, 2006). Given their low amplitude relative to the much larger cytosolic contractile Ca^{2+} these transients have been difficult to characterize (Berridge, 2006; Berridge et al., 2003). Here we show signaling Ca^{2+} changes in different cellular compartments of cultured, non-beating adult rat ventricular myocyte (ARVM) stimulated by NE. ARVMs are commonly used to study cardiac growth, apoptosis, and SR stress (Ellingsen et al., 1993), representing a useful model system to test methods for Ca^{2+} measurements.

The development of the genetically encoded calcium indicators (GECI) can be affected by two major pitfalls: First, the subcellular targeting of the probe can be challenging and second, the response range of the probe may not match the reported *in vitro* values (Filippin et al., 2005; O'Malley et al., 1999). In our experiments, the targeting was particularly difficult in the case of the mitochondrial probe, where a single targeting sequence proved to be insufficient for the correct probe localization. In fact, quadrupling of the subunit VIII COX targeting sequence was necessary to ensure any mitochondrial localization. A similar approach to mitochondrial targeting of a different probe was described previously (Filippin et al., 2005; Wüst et al., 2017).

In all four subcellular localizations, the measured intracellular K_d was different from the *in vitro* reported K_d value (Fig. 4). This difference likely results from the different molecularly dense microenvironments (O'Malley et al., 1999) and could not be accurately predicted prior to the experiments. Thus, extensive iterative trials were required to arrive at appropriate *in vitro* [Ca^{2+}] sensitivities. Nevertheless, our measured K_d values are consistent with the prior literature for each cellular subcompartment. The calibration of both cytosolic (measured EC50 73 ± 3.5 nM) and mitochondrial (measured EC50 91 ± 6 nM) probes

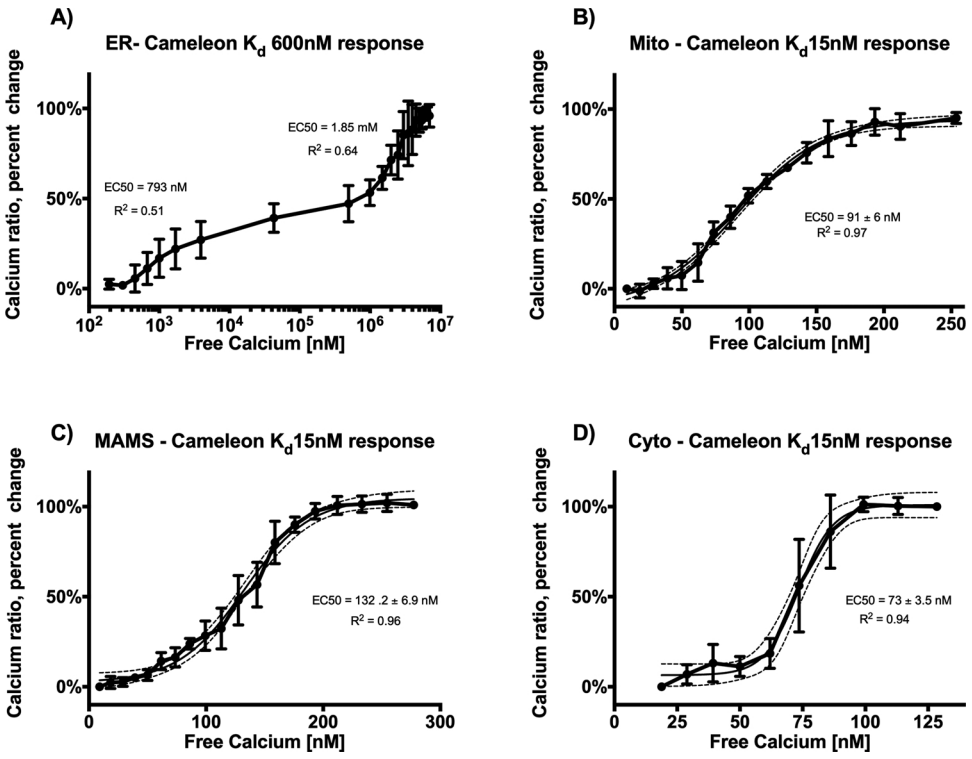

Fig. 4. Calibration of the Cameleon probes. For calibration, cardiomyocytes were incubated in a potassium phosphate Hepes buffer with BAPTA 5 nM and set at pH = 7.4 for cytosolic, SR and MAM probes (**Panel A, C, D)** and pH = 8 for mitochondrial probe (**Panel B**) to mimic pH in mitochondrial matrix. Ionomycin (5 u M) was added to permeabilize the membranes and to determine R_{min}. Small volumes of $CaCl_2$ were added in stepwise manner to generate the calibration curve until the R_{max} was reached. After conversion of the x-axis to logarithmic scale, the dose-response curve was fitted using GraphPad Prism software and 50% effective $[Ca^{2+}]$ (EC50) was calculated for each probe. Fitted curves shown with ± 95% confidence interval boundaries (n = 3–4 for each calibration).

proved that each of K_d values are within the expected range of previously reported $[Ca^{2+}]$ for the respective compartment (Raffaello et al., 2016; Wüst et al., 2017). Similarly, the K_d of the SR probe, with its double dissociation constant as detected by our calibration (with higher EC50 at 1.85 mM) falls into the previously reported range as well (Greotti et al., 2016; Raffaello et al., 2016). The MAMs probe calibration revealed a cellular K_d higher than the cytosolic probe (EC50 132.2 ± 6.9 nM). This likely reflects a more molecularly dense environment in MAMs compared to the cytosol and also makes the probe suitable to assess higher $[Ca^{2+}]$ in proximity of "Ca^{2+} hot spots" (Giacomello et al., 2010).

In the sarcoplasmic reticulum, NE increased $[Ca^{2+}]$, as expected. This effect was mostly due to beta-adrenergic stimulation, although there may have been a small contribution from alpha-adrenergic stimulation as there was complete attenuation when both beta- and alpha-receptors were blocked. The beta-adrenergic rise in SR calcium was likely due to activation of influx via SERCA. A small alpha-receptor mediated effect may reflect influx via store operated channels (Bartoli and Sabourin, 2017).

In mitochondria, calcium concentrations as high as 600 nM have been estimated in contracting cardiac myocytes during systole (Wüst et al., 2017; Zaglia et al., 2017). Since our cells were not contracting, systolic flux of calcium from the cytosol was absent, thus resulting in the lower measured $[Ca^{2+}]$. Additionally, since Cameleon probes respond to free Ca^{2+}, and much of the mitochondrial Ca^{2+} is buffered (Coll et al., 1982; Wei et al., 2012), our results fall on the lower end of the previously published $[Ca^{2+}]$ range. The calibration of the mitochondrial probe (measured EC50 91 ± 6 nM) suggests that $[Ca^{2+}]_{mito}$ in our model ranges between 60–150 nM, which is consistent with previously published data (Wüst et al., 2017). NE stimulated an increase in mitochondrial $[Ca^{2+}]$. Similar to the SR, in mitochondria, the effect of NE was largely blocked by propranolol, with some further inhibition with the addition of prazosin, suggesting that the increase was mediated primarily by the beta-adrenergic signaling. Unlike the SR, the increase in mitochondrial Ca^{2+} was faster and occurred as early as 60 s after NE stimulation. This suggests a direct effect of NE on mitochondrial Ca^{2+} uptake, possibly through stimulation of the mitochondrial calcium uniporter (MCU) (Finkel et al., 2015; Pan et al., 2013; Wu et al., 2015).

In the MAM space, in contrast to mitochondria, NE decreased the $[Ca^{2+}]$. As in the SR, this effect of NE was primarily mediated by beta-receptors, although a small alpha-adrenergic component may have contributed. The MAM represents space where the SR and mitochondria are in close proximity that facilitates Ca^{2+} transfer (Csordás and Hajnóczky, 2009; Raffaello et al., 2016; Stone et al., 2009; Wang et al., 2018). The NE-stimulated increase in mitochondrial Ca^{2+} occurred rapidly over about 60 s, whereas the NE-stimulated decrease in the MAM was slower, evolving over about 10 min, a time course similar to that for the NE-stimulated increase in the SR. We found that inhibition of either SR or mitochondrial uptake attenuated the NE-induced decrease in MAM calcium. This data suggests that both the SR and mitochondria participate in regulation of MAM $[Ca^{2+}]$. These observations coupled with the differential temporal relationship suggests that the decrease in MAM $[Ca^{2+}]$ is related to interplay between SR and mitochondrial uptake. Our findings are consistent with the reports suggesting that MAM contains SERCA and represents a place of SR/mitochondrial cross-talk (Chami et al., 2008; Raffaello et al., 2016; Rizzuto et al., 1998).

5. Conclusion

In quiescent primary culture ARVM, we used genetically-targeted Cameleon probes to monitor Ca^{2+} in subcellular locations. Under conditions that had no effect on $[Ca^{2+}]$ in the cytosol, adrenergic stimulation caused directionally and temporally distinct responses in the SR, mitochondria and MAM. This targeted approach provides better understanding of the role Ca^{2+} plays in signaling, in and between these compartments in cardiac myocytes, and could be easily applicable to other primary cell culture systems as well.

Sources of funding

Supported by NIH grants HL-064750 (WSC), NIDDK R01 DK103750 (MMB), NIH CTSI award 1UL1TR001430 (MMB) and the NHLBI-

sponsored Boston University Cardiovascular Proteomics Center (Contract No. N01-HV-28178, WSC). Dr. Bachschmid was also funded by American Heart Association "Grant in Aid" 16GRNT27660006 and the Evans Junior Faculty Research Award by the Department of Medicine of Boston University. Dr Pimentel and DR Bachschmid share a Boston University School of Medicine Whitaker Cardiovascular Institute Pilot Grant. Dr. Luptak is the recipient of an AHA Fellow-to-Faculty Award 15FTF25890062.

References

Balaban, R.S., 2009. The role of Ca2+ signaling in the coordination of mitochondrial ATP production with cardiac work. Biochim. Biophys. Acta - Bioenerg. 1787, 1334–1341. https://doi.org/10.1016/j.bbabio.2009.05.011.

Bartoli, F., Sabourin, J., 2017. cardiac remodeling and disease: current understanding of STIM1/Orai1- mediated Store-operated Ca2+ entry in cardiac function and pathology. Store-Operated Ca2+ Entry (SOCE) Pathways. pp. 523–534. https://doi.org/10.1007/978-3-319-57732-6.

Baughman, J.M., Perocchi, F., Girgis, H.S., Plovanich, M., Belcher-Timme, C.A., Sancak, Y., Bao, X.R., Strittmatter, L., Goldberger, O., Bogorad, R.L., Koteliansky, V., Mootha, V.K., 2011. Integrative genomics identifies MCU as an essential component of the mitochondrial calcium uniporter. Nature 476, 341–345. https://doi.org/10.1038/nature10234.

Berridge, M.J., 2006. Calcium microdomains: organization and function. Cell Calcium 40, 405–412. https://doi.org/10.1016/j.ceca.2006.09.002.

Berridge, M.J., Bootman, M.D., Roderick, H.L., 2003. Calcium signalling: dynamics, homeostasis and remodelling. Nat. Rev. Mol. Cell Biol. 4, 517–529. https://doi.org/10.1038/nrm1155.

Bers, D.M., 2008. Calcium cycling and signaling in cardiac myocytes. Annu. Rev. Physiol. 70, 23–49. https://doi.org/10.1146/annurev.physiol.70.113006.100455.

Bers, D.M., 2002. Cardiac excitation-contraction coupling. Nature 415, 198–205. https://doi.org/10.1038/415198a.

Boyman, L., Williams, G.S.B., Khananshvili, D., Sekler, I., Lederer, W.J., 2013. NCLX: the mitochondrial sodium calcium exchanger. J. Mol. Cell. Cardiol. 59, 205–213. https://doi.org/10.1016/j.yjmcc.2013.03.012.

Boyman, L., Williams, G.S.B., Lederer, W.J., 2015. The growing importance of mitochondrial calcium in health and disease. Proc. Natl. Acad. Sci. U.S.A. 112, 11150–11151. https://doi.org/10.1073/pnas.1514284112.

Brookes, P.S., Yoon, Y., Robotham, J.L., Anders, M.W., Sheu, S.S., 2004. Calcium, ATP, and ROS: a mitochondrial love-hate triangle. Am. J. Physiol., Cell Physiol. 287, C817–C833. https://doi.org/10.1152/ajpcell.00139.2004.

Chami, M., Oulès, B., Szabadkai, G., Tacine, R., Rizzuto, R., Paterlini-Bréchot, P., 2008. Role of SERCA1 truncated isoform in the proapoptotic calcium transfer from ER to mitochondria during ER stress. Mol. Cell 32, 641–651. https://doi.org/10.1016/j.molcel.2008.11.014.

Coll, K.E., Joseph, S.K., Corkey, B.E., Williamson, J.R., 1982. Determination of the matrix free Ca2+ concentration and kinetics of Ca2+ efflux in liver and heart mitochondria. J. Biol. Chem. 257, 8696–8704.

Csordás, G., Hajnóczky, G., 2009. SR/ER-mitochondrial local communication: calcium and ROS. Biochim. Biophys. Acta - Bioenerg. 1787, 1352–1362. https://doi.org/10.1016/j.bbabio.2009.06.004.

Ellingsen, O., Davidoff, A.M.Y.J., Prasad, S.K., Marsh, J.D., Kelly, R.A., Smith, W., Davidoff, J., Springhorn, P., Smith, T.W., 1993. Adult rat ventricular myocytes cultured in defined medium: phenotype and electromechanical function. Am. J. Physiol. Hear. Circ. Physiol. 265, H747–H754. https://doi.org/10.1152/ajpheart.1993.265.2.H747.

Filippin, L., Abad, M.C., Gastaldello, S., Magalhães, P.J., Sandonà, D., Pozzan, T., 2005. Improved strategies for the delivery of GFP-based Ca2+sensors into the mitochondrial matrix. Cell Calcium 37, 129–136. https://doi.org/10.1016/j.ceca.2004.08.002.

Finkel, T., Menazza, S., Holmström, K.M., Parks, R.J., Liu, Julia, Sun, J., Liu, Jie, Pan, X., Murphy, E., 2015. The ins and outs of mitochondrial calcium. Circ. Res. 116, 1810–1819. https://doi.org/10.1161/CIRCRESAHA.116.305484.

Giacomello, M., Drago, I., Bortolozzi, M., Scorzeto, M., Gianelle, A., Pizzo, P., Pozzan, T., 2010. Ca2+ hot spots on the mitochondrial surface are generated by Ca2+ mobilization from stores, but not by activation of store-operated Ca2+ channels. Mol. Cell 38, 280–290. https://doi.org/10.1016/j.molcel.2010.04.003.

Greotti, E., Wong, A., Pozzan, T., Pendin, D., Pizzo, P., 2016. Characterization of the ER-targeted low affinity Ca2+probe D4ER. Sensors Basel (Basel) 16, 1419. https://doi.org/10.3390/s16091419.

Gustafsson, M.G.L., Shao, L., Carlton, P.M., Wang, C.J.R., Golubovskaya, I.N., Cande, W.Z., Agard, D.A., Sedat, J.W., 2008. Three-dimensional resolution doubling in wide-field fluorescence microscopy by structured illumination. Biophys. J. 94, 4957–4970. https://doi.org/10.1529/biophysj.107.120345.

Horikawa, K., Yamada, Y., Matsuda, T., Kobayashi, K., Hashimoto, M., Matsu-Ura, T., Miyawaki, A., Michikawa, T., Mikoshiba, K., Nagai, T., 2010. Spontaneous network activity visualized by ultrasensitive Ca2+indicators, yellow Cameleon-Nano. Nat. Methods 7, 729–732. https://doi.org/10.1038/nmeth.1488.

Kuster, G.M., Pimentel, D.R., Adachi, T., Ido, Y., Brenner, D.A., Cohen, R.A., Liao, R., Siwik, D.A., Colucci, W.S., 2005. Alpha-adrenergic receptor-stimulated hypertrophy in adult rat ventricular myocytes is mediated via thioredoxin-1-sensitive oxidative modification of thiols on Ras. Circulation 111, 1192–1198. https://doi.org/10.1161/01.CIR.0000157148.59308.F5.

Liu, T., O'Rourke, B., 2009. Regulation of mitochondrial Ca2+ and its effects on energetics and redox balance in normal and failing heart. J. Bioenerg. Biomembr. 41, 127–132. https://doi.org/10.1007/s10863-009-9216-8.

Luptak, I., Balschi, J.A., Xing, Y., Leone, T.C., Kelly, D.P., Tian, R., 2005. Decreased contractile and metabolic reserve in peroxisome proliferator-activated receptor-alpha-null hearts can be rescued by increasing glucose transport and utilization. Circulation 112, 2339–2346. https://doi.org/10.1161/CIRCULATIONAHA.105.534594.

Luptak, I., Sverdlov, A.L., Panagia, M., Qin, F., Pimentel, D.R., Croteau, D., Siwik, D.A., Ingwall, J.S., Bachschmid, M.M., Balschi, J.A., Colucci, W.S., 2018. Decreased ATP production and myocardial contractile reserve in metabolic heart disease. J. Mol. Cell. Cardiol. 116, 106–114. https://doi.org/10.1016/j.yjmcc.2018.01.017.

Mayourian, J., Ceholski, D.K., Gonzalez, D.M., Cashman, T.J., Sahoo, S., Hajjar, R.J., Costa, K.D., 2018. Physiologic, pathologic, and therapeutic paracrine modulation of cardiac excitation-contraction coupling. Circ. Res. 122, 167–183. https://doi.org/10.1161/CIRCRESAHA.117.311589.

Miyawaki, A., Llopis, J., Heim, R., McCaffery, J.M., Adams, J.A., Ikura, M., Tsien, R.Y., 1997. Fluorescent indicators for Ca2+ based on green fluorescent proteins and calmodulin. Nature 388, 882–887. https://doi.org/10.1038/42264.

O'Malley, D.M., Burbach, B.J., Adams, P.R., 1999. Confocal Microscopy. Humana Press Inc, Totowa, New Jersey. https://doi.org/10.1385/159259722X.

Palmer, A.E., Giacomello, M., Kortemme, T., Hires, S.A., Lev-Ram, V., Baker, D., Tsien, R.Y., 2006. Ca2+Indicators based on computationally redesigned calmodulin-peptide pairs. Chem. Biol. 13, 521–530. https://doi.org/10.1016/j.chembiol.2006.03.007.

Palmer, A.E., Tsien, R.Y., 2006. Measuring calcium signaling using genetically targetable fluorescent indicators. Nat. Protoc. 1, 1057–1065. https://doi.org/10.1038/nprot.2006.172.

Pan, X., Liu, J., Nguyen, T., Liu, C., Sun, J., Teng, Y., Fergusson, M.M., Rovira, I.I., Allen, M., Springer, D.A., Aponte, A.M., Gucek, M., Balaban, R.S., Murphy, E., Finkel, T., 2013. The physiological role of mitochondrial calcium revealed by mice lacking the mitochondrial calcium uniporter. Nat. Cell Biol. 15, 1464–1472. https://doi.org/10.1038/ncb2868.

Paredes, R.M., Etzler, J.C., Watts, L.T., Zheng, W., Lechleiter, J.D., 2008. Chemical calcium indicators. Methods 46, 143–151. https://doi.org/10.1016/j.ymeth.2008.09.025.

Pimentel, D.R., Adachi, T., Ido, Y., Heibeck, T., Jiang, B., Lee, Y., Melendez, J.A., Cohen, R.A., Colucci, W.S., 2006. Strain-stimulated hypertrophy in cardiac myocytes is mediated by reactive oxygen species-dependent Ras S-glutathiolation. J. Mol. Cell. Cardiol. 41, 613–622. https://doi.org/10.1016/j.yjmcc.2006.05.009.

Raffaello, A., Mammucari, C., Gherardi, G., Rizzuto, R., 2016. Calcium at the center of cell signaling: interplay between endoplasmic reticulum, mitochondria, and lysosomes. Trends Biochem. Sci. 41, 1035–1049. https://doi.org/10.1016/j.tibs.2016.09.001.

Rasmussen, T.P., Wu, Y., Joiner, M.A., Koval, O.M., Wilson, N.R., Luczak, E.D., Wang, Q., Chen, B., Gao, Z., Zhu, Z., Wagner, B.A., Soto, J., McCormick, M.L., Kutschke, W., Weiss, R.M., Yu, L., Boudreau, R.L., Abel, E.D., Zhan, F., Spitz, D.R., Buettner, G.R., Song, L.-S., Zingman, L.V., Anderson, M.E., 2015. Inhibition of MCU forces extramitochondrial adaptations governing physiological and pathological stress responses in heart. Proc. Natl. Acad. Sci. U.S.A. 112, 9129–9134. https://doi.org/10.1073/pnas.1504705112.

Rizzuto, R., Pinton, P., Carrington, W., Fay, F.S., Fogarty, K.E., Lifshitz, L.M., Tuft, R.A., Pozzan, T., 1998. Close contacts with the endoplasmic reticulum as determinants of mitochondrial Ca 2+ responses. Science 280, 1763–1766. https://doi.org/10.1126/science.280.5370.1763.

Santulli, G., Xie, W., Reiken, S.R., Marks, A.R., 2015. Mitochondrial calcium overload is a key determinant in heart failure. Proc. Natl. Acad. Sci. U. S. A. 112, 11389–11394. https://doi.org/10.1073/pnas.1513047112.

Stone, S.J., Levin, M.C., Zhou, P., Han, J., Walther, T.C., Farese, R.V., 2009. The endoplasmic reticulum enzyme DGAT2 is found in mitochondria-associated membranes and has a mitochondrial targeting signal that promotes its association with mitochondria. J. Biol. Chem. 284, 5352–5361. https://doi.org/10.1074/jbc.M805768200.

Wang, W., Fernandez-Sanz, C., Sheu, S.S., 2018. Regulation of mitochondrial bioenergetics by the non-canonical roles of mitochondrial dynamics proteins in the heart. Biochim. Biophys. Acta Mol. Basis Dis. 1864, 1991–2001. https://doi.org/10.1016/j.bbadis.2017.09.004.

Wei, A.-C., Liu, T., Winslow, R.L., O'Rourke, B., 2012. Dynamics of matrix-free Ca $^{2+}$ in cardiac mitochondria: two components of Ca^{2+} uptake and role of phosphate buffering. J. Gen. Physiol. 139, 465–478. https://doi.org/10.1085/jgp.201210784.

Wu, Y., Rasmussen, T.P., Koval, O.M., Joiner, M.L.A., Hall, D.D., Chen, B., Luczak, E.D., Wang, Q., Rokita, A.G., Wehrens, X.H.T., Song, L.S., Anderson, M.E., 2015. The mitochondrial uniporter controls fight or flight heart rate increases. Nat. Commun. 6, 6081. https://doi.org/10.1038/ncomms7081.

Wüst, R.C., Helmes, M., Martin, J.L., van der Wardt, T.J., Musters, R.J., van der Velden, J., Stienen, G.J., 2017. Rapid frequency-dependent changes in free mitochondrial calcium concentration in rat cardiac myocytes. J. Physiol. (Paris) 595, 2001–2019. https://doi.org/10.1113/JP273589.

Zaglia, T., Ceriotti, P., Campo, A., Borile, G., Armani, A., Carullo, P., Prando, V., Coppini, R., Vida, V., Stølen, T.O., Ulrik, W., Cerbai, E., Stellin, G., Faggian, G., De Stefani, D., Sandri, M., Rizzuto, R., Di Lisa, F., Pozzan, T., Catalucci, D., Mongillo, M., 2017. Content of mitochondrial calcium uniporter (MCU) in cardiomyocytes is regulated by microRNA-1 in physiologic and pathologic hypertrophy. Proc. Natl. Acad. Sci. U.S.A. 114, E9006–E9015. https://doi.org/10.1073/pnas.1708772114.